Remote Axial Tuning in Microscopy Utilizing Hydrogel-Driven Tunable Liquid Lens

Aditi Kanhere, Guangyun Lin, and Hongrui Jiang, *Senior Member, IEEE*

***Abstract*— This paper presents the use of a tunable-focus thermoresponsive hydrogel-based liquid lens in combination with an objective lens to achieve remote axial focusing in conventional microscopy. The goal of this design is to eliminate image distortion due to sample vibrations caused by mechanical stage scanning. This approach reduces the mechanical complexity and power consumption due to the use of electrically tunable lenses, while achieving a twofold increase in the axial scanning range. The merits of the proposed design were demonstrated by characterizing a customized microscope system over a scanning range of 1700 μm. A lateral resolution of 2 μm was obtained consistently throughout the scanning range. Healthy *Spodoptera frugiperda* Sf21 insect cells imaging was used to verify the depth scanning ability and the resolution of our remote focusing microscope system. [2015-0282]**

***Index Terms*— Tunable lenses, microscopy, axial tuning.**

I. Introduction

CONVENTIONAL wide-field microscopy is one of the most widely used optical microscopy technique. This technique typically captures a two-dimensional image of a specimen. However, many applications such as diagnostic microfluidic applications [1], tissue sampling [2] or multi-layered microfluidic samples [3] require a volumetric scan. To enable a volumetric visualization of the sample it is necessary to move the sample, relative to the fixed focal plane of the microscope objective, along the axial direction. For this purpose, a mechanical z-scanning stage is typically employed to enable linear translation along the depth of the sample. The stage enables a controlled shift of the focal plane through different layers of the sample. Typical approaches used to achieve such axial scanning employ a motorized stepper stage or a piezoelectric stage to move the sample along the z-axis. While stepper motors offer the advantage of unlimited travel distance, they suffer from hysteresis. Piezoelectric stages on the other hand, help eliminate hysteresis at the cost of the travel distance which is reduced to 100-200 μm. Both types of stages, however, are bulky and cause vibrations and wobble in the sample due to high inertia. Additional care is required to avoid mechanical overshoots and backlash from the tip touching the sample [4]. Additionally, for water or oil-immersion lenses, vibration of the sample stage can cause disturbance or ripples in the immersion media that can lead to significant distortion in the images.

A robust alternative to the use of mechanical scanning stages is a remote axial focusing system that allows both the objective and the sample to be stationary. One way to achieve this is the employment of a tunable-focus lens in the imaging path to achieve shift of the axial position of the native focal plane of the microscope through different depths of the specimen being imaged. Several groups have reported the implementation of tunable-focus lenses for depth scanning in different microscopy techniques, including fast axial focusing in two-photon microscopy [5], optical coherence microscopy [6], optical tweezers [7] and light-sheet microscopy [8]. Koukourakis *et al.* previously presented their proof-of-principle work showing the utility of adaptive lenses for axial focusing in confocal microscopy [9]. Other research groups have used electrically tunable lenses based on polymer membrane-liquid interface as well as electro-wetting based liquid lenses to achieve volumetric scanning [10]–[12]. However, most of these techniques either require high driving voltages or can achieve a unidirectional axial focal shift and need to be combined with an offset lens to focus symmetrically above and below the native focal plane. Adding optical components requires a higher precision in alignment as well as contributes to optical aberrations. Using the aforementioned solutions, an axial tuning range of 700 μm or less can be achieved.

We propose a compact, energy and cost-efficient solution for remote axial focusing using thermo-responsive hydrogel based liquid lenses that can achieve scanning over 1700 μm, which is a two-fold increase in the previously reported values for axial scan in conventional microscopy. Hydrogel-based liquid lenses offer a high degree of flexibility in terms of tuning temperature range, direction and magnitude of the axial focus scan. We characterized the system using optical models in ZEMAX and imaging microspheres suspended in stacked microfluidic channels. A resolution of 2 μm or better was observed across all values of attainable focal scans. Healthy *Spodoptera frugiperda* Sf21 insect cells were imaged to verify the axial focusing functionality of the optical system.

II. Experimental

A. Principle of Operation

The work presented here is developed on the key idea that a focus-tunable liquid lens when introduced in the optical path

Manuscript received October 13, 2015; revised January 4, 2016; accepted January 14, 2016. Date of publication February 3, 2016; date of current version March 31, 2016. This work was supported by the U.S. National Institutes of Health under Grant 1DP2OD008678-01. Subject Editor J. A. Yeh.

A. Kanhere is with Digilens Inc., Sunnyvale, CA 94089 USA (e-mail: aditi1812@gmail.com).

G. Lin is with the Department of Electrical and Computer Engineering, University of Wisconsin–Madison, Madison, WI 53706 USA (e-mail: glin2@wisc.edu).

H. Jiang is with the Department of Electrical and Computer Engineering, Department of Materials Science and Engineering, Department of Biomedical Engineering, and the McPherson Eye Research Institute, University of Wisconsin-Madison, Madison, WI 53706 USA (e-mail: hongrui@engr.wisc.edu).

Color versions of one or more of the figures in this paper are available online at http://ieeexplore.ieee.org.

Digital Object Identifier 10.1109/JMEMS.2016.2518922

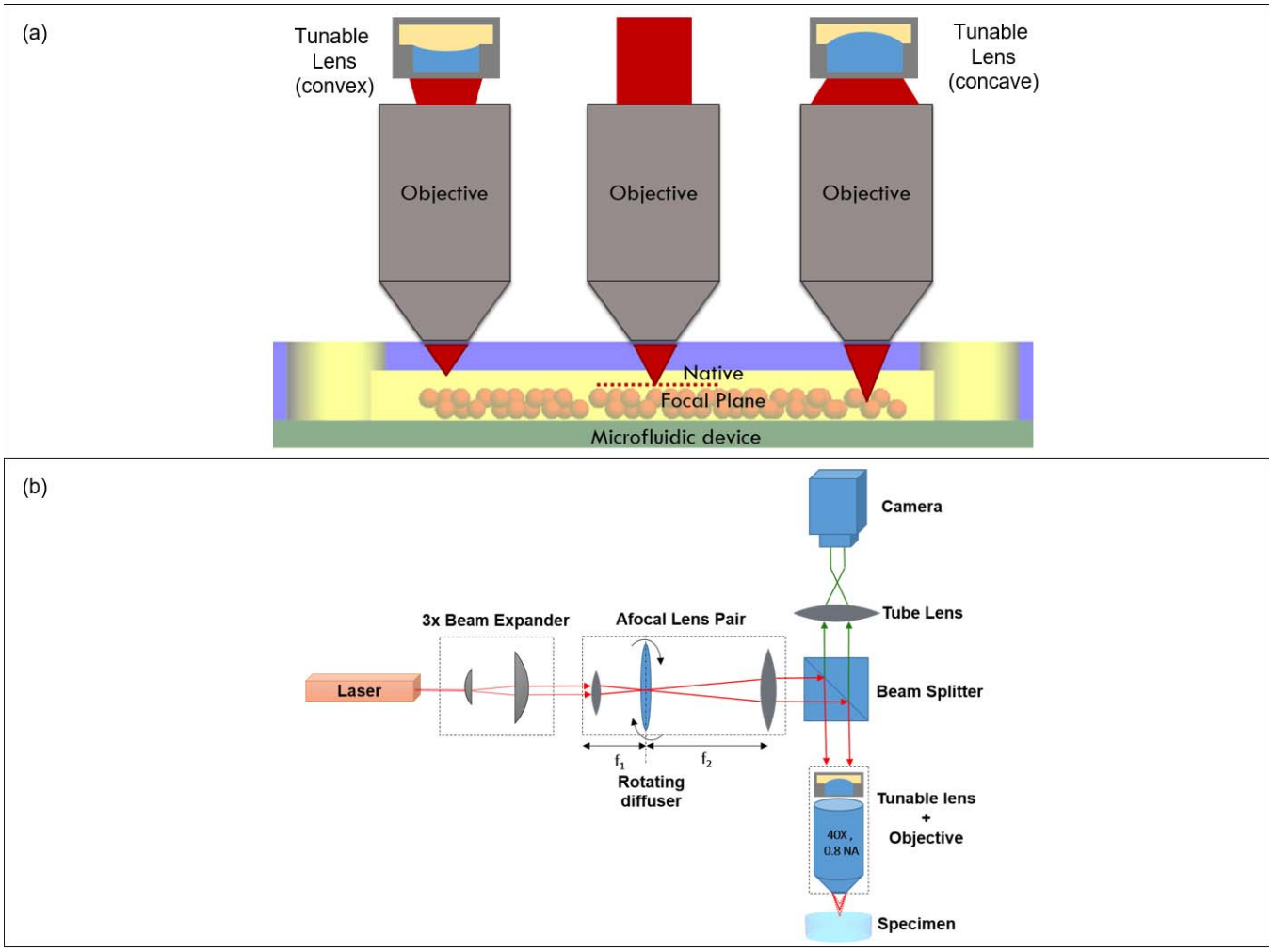

Fig. 1. (a) Schematic illustrating the operating principle of a 3D microscope with remote axial focusing achieved with tunable-focus liquid lenses. As the focal length of the lens placed behind an objective lens changes, it alters the divergence of the incident beam to shift the native focal plane of the objective lens. The direction of the axial shift depends on the degree of divergence or convergence of the incident beam. (b) Optical ray diagram and 3D schematic of the actual setup of the microscope. An incident laser expanded to the desired beam diameter is deflected onto a tunable-focus lens and objective lens combination. The focal plane of the microscope is scanned along the axial direction as the focal length of the tunable lens changes. The detection arm consists of a tube lens and a camera to record the image.

of a microscope will alter the position of the native focal plane within a sample. When the tunable liquid lens is placed behind the microscope objective, the lens alters the divergence of the incident beam as its focal length changes. The result is a shift in the position of the focal plane along the axial direction (optical axis). The direction and magnitude of the axial shift are dependent on the focal length of the lens and the distance between the tunable lens and objective lens. When the beam incident on the objective is convergent, the native focal plane will shift towards the objective along the optical axis. On the other hand, diverging the incident beam will shift the focal plane further away from the objective in the axial direction. In other words, a convex lens in conjunction with the objective will reduce, and a concave lens will increase the working distance of the microscope. We can use this phenomenon of remote axial focusing to image through different depths of a sample without the need for a mechanical axial translation stage. Fig. 1(a) shows a schematic to illustrate the principle of operation of our optical system.

The focus-tunable liquid lenses used in our system are hydrogel based liquid lenses whose focal length can be varied by changing the ambient temperature. The lens is defined by an interface between two immiscible optical liquids with different refractive indices but closely matched densities, typically water and oil. The lens meniscus is manipulated by changing the volume of water on one side of a pinned liquid-liquid interface. This change in volume is achieved by expansion or shrinkage of a smart hydrogel ring structure surrounding the water chamber, in response to an ambient temperature change. The lens design is similar to the hydrogel-based tunable lenses reported in our previous publications [13]–[15].

B. Optical Setup

A 632.8 nm randomly polarized laser (HNL050R, Thorlabs Inc., Newton, NJ) is used for illumination. The output power of the laser is 5mW with a beam diameter ($1/e^2$) of 0.81 mm. The beam expander stage comprises of a commercial 3× beam expander (BE03M-A, Thorlabs Inc., Newton, NJ)

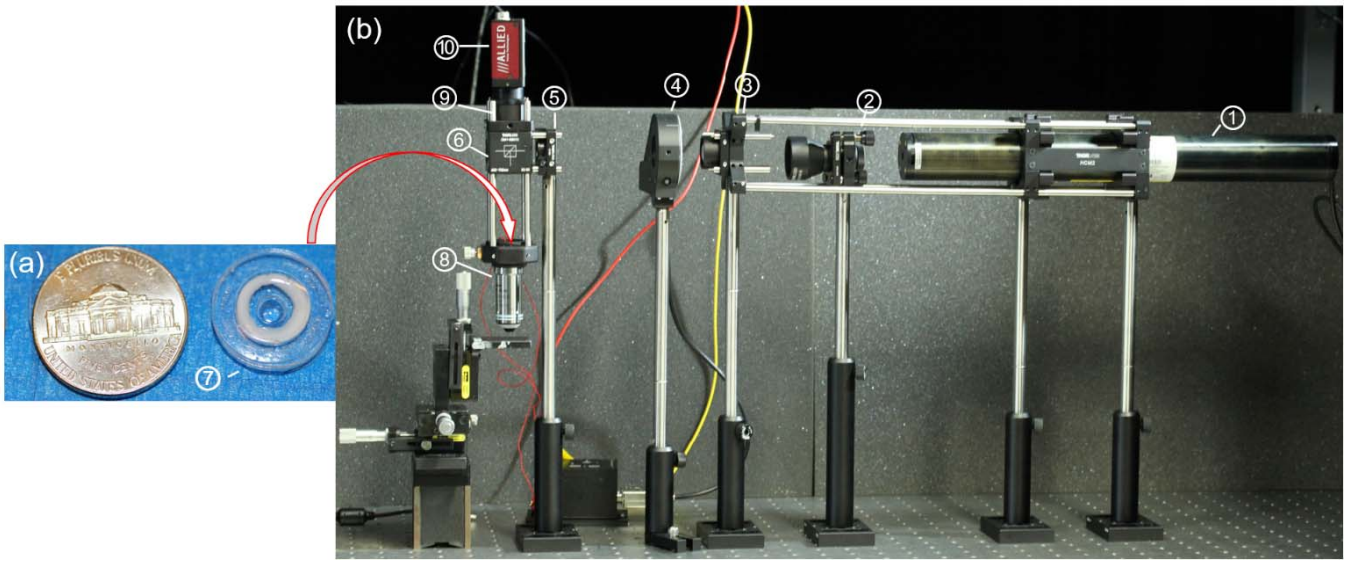

Fig. 2. Optical setup of a microscope with (a) a thermo-responsive hydrogel-based tunable lens used for remote axial focusing. (b) A laser beam (①) is first expanded using a beam expander (②, ③, ⑤). A rotating diffuser (④) is used to reduce coherence of the light source. A beamsplitter (⑥) then deflects the beam onto a tunable lens (⑦) placed close to the rear stop of an objective lens (⑧). Images at different axial depths of a sample, achieved by tuning the liquid lens are then focused onto an image sensor (⑨) with a tube lens (⑩).

and a 3.33× afocal lens pair (AC254-030-A and AC254-100-A, Thorlabs Inc., Newton, NJ). The beam expansion stage is designed to ensure that the size of the beam incident on the microscope objective is greater than the pupil diameter (8mm). This is essential to ensure uniform illumination of the objective and hence optimal imaging. To reduce the spatial coherence of the laser beam, a rotating optical diffuser is placed in the Fourier plane of the afocal lens pair after the beam expander. The expanded beam is then passed through an adjustable iris diaphragm before being deflected onto the tunable lens using a beam splitter. The variable iris/aperture controls the width of the bundle of light rays to eliminate excess light that can cause glare and reduce contrast. A 4-mm-aperture tunable lens is used to alter the beam divergence at the back focal plane of a water-immersion microscope objective (CFI Apo 40XW NIR, Nikon). The tunable lens is mounted in a custom PDMS alignment ring placed within an *x-y* translation mount and is encapsulated in an insulated, flexible polyimide heater with a power density of 10 W/in2 at 28V (Kapton KHLV-0502/10, Omega Engineering Inc., Stamford, CT, USA) to vary the lens temperature. The *x-y* translation mount facilitates precise centering of the tunable lens with the optical axis of the objective which is critical to avoid lateral shifts in the image of the sample. The detection arm consists of a lens (AC254-200-A, Thorlabs Inc., Newton, NJ, USA) focusing light onto an image sensor (AVT Stingray IEEE1394 C-Mount Cameras, Allied Vision). Fig. 1(b) shows a ray tracing diagram of the optical setup of the custom microscope with remote axial focusing. Fig. 2 is a schematic of the actual setup with an inset showing the positioning of the tunable lens in the microscope.

C. Optical Modeling

We used the ZEMAX (Bellevue, WA, USA) software package to simulate light propagation through the custom microscope and to test characterize its performance. The tunable lens-objective lens combination was modelled using sequential ray tracing. The multi-configuration editor was used to define the different radii of curvature of the liquid lens corresponding to different focal lengths at different temperatures. To simulate the pinning of the liquid-liquid lens interface, an edge thickness constraint was placed on surfaces on either side of the lens surface, as shown in Fig. 3.

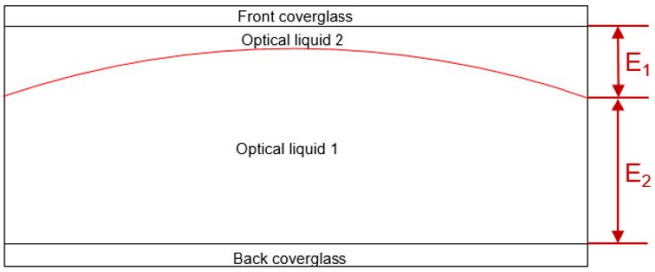

	Optical liquid 1 (Water)	Optical liquid 2 (Oil-like immersion liquid)
n	1.33	1.5
Vd	55.74	41.6
Density	1g/cm^3	0.894 g/cm^3

Fig. 3. Optical model of the tunable liquid lens. To simulate a pinned liquidliquid interface, the edge thicknesses (E_1 and E_2) of the surfaces on the either side of the lens meniscus were constrained. Typically used silicone oil (Optical liquid 2) was replaced with an oil-like immersion liquid with a refractive index equal to that of the front cover glass of the lens, to reduce refractive index mismatch.

The widths and thicknesses of the liquid chambers were optimized using a merit function to minimize the RMS spot size at the image plane. Due to lack of prescription data for the commercial objective lens, we used the data from a patent [16] to model the water immersion microscope objective as accurately as possible. The modelled objective has

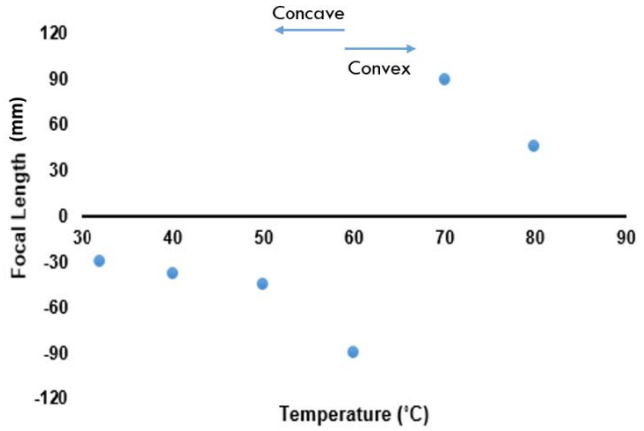

Fig. 4. Focal length variations of a sample tunable liquid lens with change in ambient temperature. The initial volume of water was adjusted so that the tunable lens is concave with a focal length of −30mm. As the temperature increases above a critical temperature (32°C), the focal length decreases. At a certain temperature, the lens tunes through ∞ and snaps to a convex lens and the focal length continues to decrease.

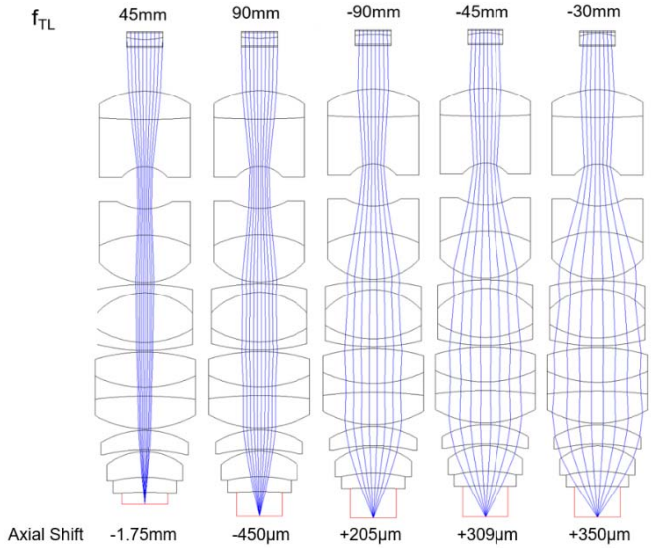

Fig. 5. Optical layouts illustrating the shift in axial position of the native focal plane of the microscope with changing focal length of the tunable lens. The positive values of the shift indicate a shift of the focal plane towards the front end of the objective lens and the negative values correspond to a shift away from the objective lens. The simulated value of the axial shift is 2.1 mm which is consistent with the measured axial shift value of 1.7 mm.

a working distance of 3.3 mm which differs slightly from the actual working distance of 3.5 mm of the commercial objective lens.

III. Results and Discussion

A. Lens Calibration

The lens design can be easily adapted for different ranges of attainable focal lengths. This can be achieved by changing the initial water volume filled in the water chamber at room temperature. For our experiments reported in this work, the lenses were designed to tune from focal lengths of −30 mm to −∞ and from 45 mm to +∞. The focal length variations with changing temperature as recorded for one such tunable lens have been plotted in Fig. 4. By changing the initial water volume, the axial tuning range can be adjusted to obtain images either from a symmetric focal shift on both sides of the native focal plane or only on one side of the native focal plane. This gives our system an added degree of flexibility and adaptability for imaging systems designed for different biological systems.

B. Characterization

1) Axial Tuning Range and Field of View: To estimate the axial tuning range of the microscope, the optical model in ZEMAX was used to calculate the focal plane shift obtained by focusing the tunable lens. The tunable lens was configured to tune through focal lengths equal to five different experimentally obtained data points shown in Fig. 5. For each configuration of the tunable lens, the new focal plane of the microscope was assumed to coincide with the axial distance at which the RMS spot size of the point image of a collimated laser beam was minimum. The axial shift is given by the distance between the new focusing distance of the microscope and the native focal plane. Fig. 5 shows the optical layouts of the setup for five different focal lengths of the tunable lens with the corresponding axial shifts. Tuning of the hydrogel-driven lens in a full back-and-forth cycle takes tens of seconds.

The setup used to measure the axial resolution of our microscope comprised of a USAF 1951 resolution target (Edmund Optics Inc., Barrington, NJ) used as an imaging sample placed on a precision Z-axis translation stage (MT3, Thorlabs Inc., Newton, NJ). The sample was initially positioned 3.5 mm away from the front end of the objective which corresponds to the native focal plane. The axial position of the target was then varied by ±1 mm with respect to the native focal plane of the microscope, in steps of 50 μm. At each step, the focal length of the liquid lens was changed to test for capability to focus the target at the new axial distance. The axial focusing range was experimentally measured to be 1.7 mm.

A distinct advantage of hydrogel-based tunable lenses is the easy adaptability of the design to obtain different values of axial tuning range and direction of the tuning with respect to the native focal plane. Typical alternative solutions using electrowetting based liquid lenses suffer from the need for much higher power compared to hydrogel-based lenses to achieve the same focal length tuning range. On the other hand, most electrically tuned lenses need to be paired with an offset lens to shift the focal plane bidirectionally with respect to the native focal plane.

To demonstrate the remote axial tuning capabilities of our system, we imaged microspheres suspended in a microfluidic device comprising of two orthogonal microfluidic channels stacked on top of each other, as shown in Fig. 6. A 0.15 mm thick coverslip is placed on top of the device. Both the microfluidic channels are 250 μm wide and 250 μm deep and are separated by a 100-μm layer of PDMS. 20 μm ± 0.3 μm diameter polystyrene microspheres (Sigma-Aldrich Co., St. Louis, MO) were suspended in the lower microfluidic

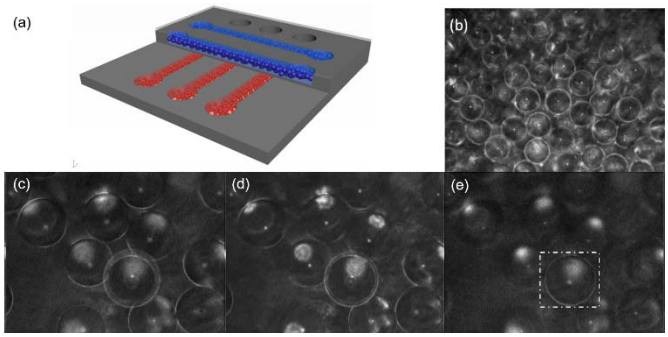

Fig. 6. Demonstration of remote axial focusing in the 3D microscope using images of a microfluidic device. (a) Schematic of the microfluidic device made up of two stacked orthogonal microfluidic channels, each 250 μm wide and 250 μm deep. 20 μm and 40 μm microspheres are suspended in lower and upper channels respectively. At the start, the focal plane of the microscope is aligned with the base of the device, then axial focusing is implemented to image upwards through different depths of the device. (b) The focal plane first shifts through the lower microfluidic channels to obtain images of the 20 μm beads. (c)-(e) As the focal plane continues to shift upwards, the microscope is able to focus on different layers of 40 μm beads within the upper microfluidic channel. The focus gradually shifts from a lower layer of beads in (c) to a highlighted bead sitting atop this layer in (e). All images have been cropped to the same field of view for ease of comparison of images captured at different axial dChange in field of view with varying axial depths due to non-telecentricity of the optical setup.

TABLE I

CHANGE IN FIELD OF VIEW WITH VARYING AXIAL DEPTHS DUE TO NONTELECENTRICITY OF THE OPTICAL SETUP

Axial shift	Field of view (Simulated)	Field of View (Experimental)
1250µm	240µm	270µm
-500µm	300µm	315µm
0	625µm (Field of view of Objective)	
200µm	400µm	380µm
400µm	435µm	400µm

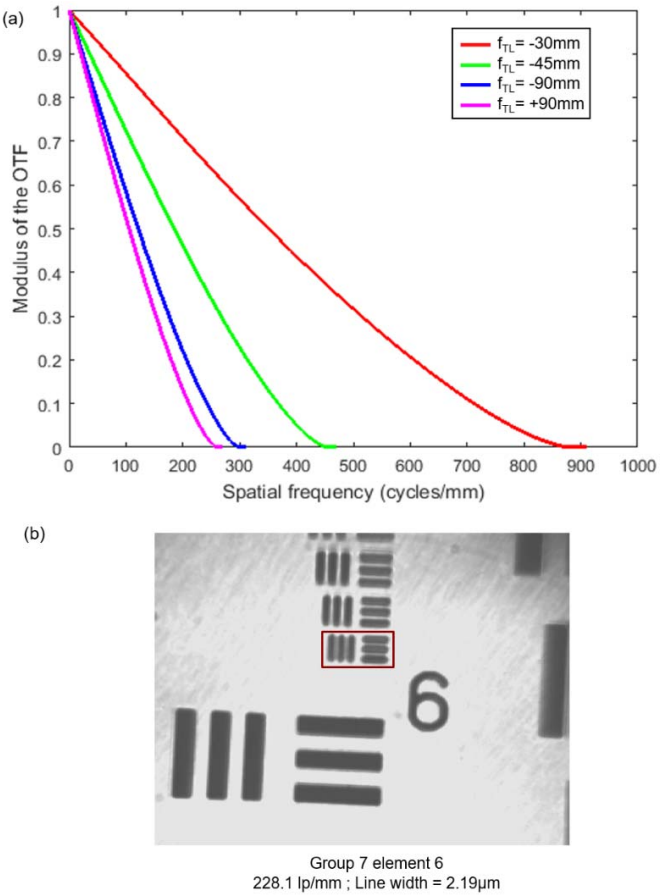

Fig. 7. (a) MTF plots of the optical system at different focal lengths of the tunable lens. The performance of the system deteriorates with increasing focal lengths. However objects with 200 lp/mm spatial frequency can be imaged with a reasonable contrast throughout the focusing range. (b) An image of a 1951 USAF resolution target as seen by the microscope. The smallest element discernible by the system has 228.1 lp/mm, which is close to the estimated resolution limit of the system.

channel whereas the upper microfluidic channel consists of 40 μm $\pm$ 0.3 μm diameter polymethacrylate microspheres (Sigma-Aldrich Co., St. Louis, MO). To image the entire microfluidic sample, we needed to achieve an axial focusing shift of 750 μm from the top of the specimen. For this, temperature of the tunable lens was varied from 55°C to 80°C to obtain focal lengths between 90 mm and -30 mm.

In our setup, the tunable lens is placed at a finite distance (5 mm) behind the rearstop of the microscope objective which lies inside the mounting shoulder and is inaccessible. As a result, the system has an angular (non-constant) field of view. In other words, the system is non-telecentric and exhibits different fields of view at different axial positions. Another interpretation of this is that the numerical aperture of the system changes as the axial position of the focal plane is changed. To characterize the effects of non-telecentricity in our imaging setup, we measured the fields of view both experimentally and in ZEMAX for different curvatures of the liquid lens.

Table 1 summarizes the simulated and experimental field of view variations with respect to various axial focus positions.

2) Aberrations and Resolution: A widely accepted measure to characterize the resolution and performance of a microscope is the Modulation Transfer Function (MTF). MTF is a measure of the ability of a microscope to transfer contrast from the specimen to the intermediate image plane at a specific resolution. Fig. 7(a) shows the diffraction MTF plots of our microscope at different focal lengths of the tunable lens, as simulated in ZEMAX.

An object imaged with a 20% contrast (MTF20) can be recovered with reasonable fidelity with standard image processing techniques. Throughout the axial scanning range, our optical microscope can image objects with a spatial frequency of 200 line pairs /mm (lp/mm) at 20% contrast or more. To compare the simulated results with experimental observations, an image of the 1951 USAF resolution target was captured with the tunable lens tuned to the focal length of $+45$ mm. Element 6 in Group 7 with a resolution of 2.19 μm or a spatial frequency of 238.1 lp/mm is clearly discernible with a reasonable contrast.

Spherical aberrations as estimated by the optical model in ZEMAX are summarized in Table 2. As the focal plane shifts closer to the front end of the objective lens, the numerical

TABLE II
SPHERICAL ABERRATIONS OF THE MICROSCOPE AS SIMULATED IN ZEMAX

	Focal length of tunable lens			
	-30mm	-45mm	-90mm	90mm
Spherical Aberrations (μm)	0.7	0.9	1.8	4.6

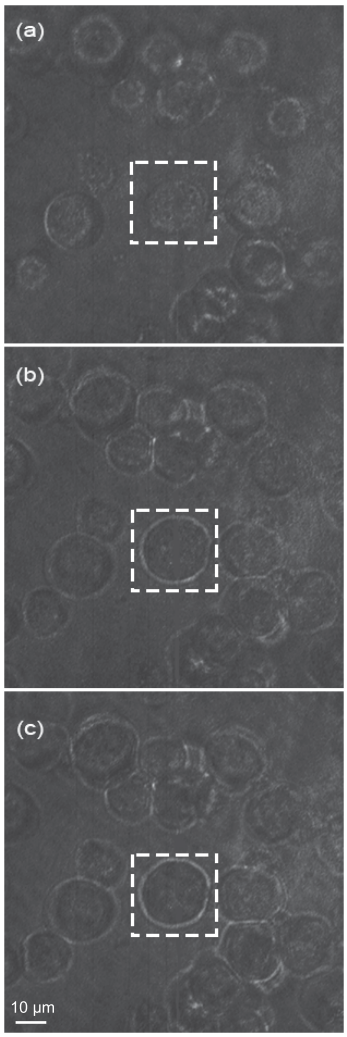

Fig. 8. Imaging SF21 cells using a microscope with remote axial focusing. A cell (highlighted) is tracked across images captured at different depths of the specimen by shifting the axial focal plane of the microscope. The cell gradually comes into focus from (a) to (c) where the membrane of the cell is clearly visible which validates our claim of a lateral resolution $\sim$2 μm.

aperture decreases and hence the resolution degrades and the aberration values increase. This effect can be verified in both the MTF plots as well as the aberration values in Table 2.

C. Live Cell Imaging

To demonstrate the operation of our microscope, we imaged Sf21 cells suspended in a microfluidic channel. The sample contained cells with an average size of 15-18 μm and a cell density of 1×10^6 cell/ml (Fig. 8). The cells were pipetted into a microfluidic chamber and a 0.15-mm-thick coverslip was placed on top of the sample to enable imaging with a water-immersion objective. The temperature of the lens was varied from 40°C to 70°C. Three images of the sample were captured at three different focal planes to demonstrate the ability to focus at different depths within the sample. The images obtained from the image sensor were then post-processed in MATLAB to enhance the contrast.

IV. CONCLUSIONS

Our work demonstrates that remote axial focusing can be implemented in a conventional microscope using hydrogel-based focus-tunable liquid lenses. A lateral resolution of 2 μm was recorded over the entire attainable axial tuning range of 1500 μm. The reported technique can be easily adapted for various combinations of magnitude and direction of the axial scan ranges and does not require complex mechanical and electrical controls. The customized microscope is a non-telecentric system and hence it suffers from a varying field of view with respect to axial distance. In its current configuration, the system suffers due to the lack of accuracy and relatively slow speed of focusing of the tunable lens, making it preferable for static samples. Future work will focus on addressing these shortcomings and will also include designing a telecentric system. The imaging resolution will also be improved in future work with better imager and more advanced image processing algorithm. Additional work will focus on evaluation and enhancement of system performance in response to a white light source. A comprehensive comparison will also be performed to compare the placement of the tunable lens in the detection arm in contrast with its placement in the imaging arm as in the current system.

ACKNOWLEDGMENT

The authors would like to thank Professor Paul Friesen and his research group at the University of Wisconsin-Madison for providing samples of cultured Sf21 cells for the imaging experiments. They would also like to thank Dr Mohammad Moghimi for discussions and guidance.

REFERENCES

[1] F. Merola, P. Memmolo, L. Miccio, V. Bianco, M. Paturzo, and P. Ferraro, "Diagnostic tools for lab-on-chip applications based on coherent imaging microscopy," *Proc. IEEE*, vol. 103, no. 2, pp. 192–204, Feb. 2015.

[2] X. Chen, B. Zheng, and H. Liu, "Optical and digital microscopic imaging techniques and applications in pathology," *Anal. Cellular Pathol.*, vol. 34, nos. 1–2, pp. 5–18, 2011.

[3] G. B. Salieb-Beugelaar, G. Simone, A. Arora, A. Philippi, and A. Manz, "Latest developments in microfluidic cell biology and analysis systems," *Anal. Chem.*, vol. 82, no. 12, pp. 4848–4864, 2010.

[4] J. A. Stroscio and W. J. Kaiser, *Scanning Tunneling Microscopy*. Boston, MA, USA: Academic, 1993.

[5] K.-S. Lee, P. Vanderwall, and J. P. Rolland, "Two-photon microscopy with dynamic focusing objective using a liquid lens," *Proc. SPIE*, vol. 7569, pp. 1–7, Feb. 2010.

[6] S. Murali, K. P. Thompson, and J. P. Rolland, "Three-dimensional adaptive microscopy using embedded liquid lens," *Opt. Lett.*, vol. 34, no. 2, pp. 145–147, 2009.

[7] *Optical Focusing in Microscopy With Optotune's Focus Tunable Lens EL-10-30*, Application Note, Optotune AG, Dietikon, Switzerland, 2011.

[8] F. O. Fahrbach, F. F. Voigt, B. Schmid, F. Helmchen, and J. Huisken, "Rapid 3D light-sheet microscopy with a tunable lens," *Opt. Exp.*, vol. 21, no. 18, pp. 21010–21026, 2013.
[9] N. Koukourakis *et al.*, "Effects of axial scanning in confocal microscopy employing adaptive lenses (CAL)," *Proc. SPIE*, vol. 9132, p. 91320P, May 2014.
[10] S. Liu and H. Hua, "Extended depth-of-field microscopic imaging with a variable focus microscope objective," *Opt. Exp.*, vol. 19, no. 1, pp. 353–362, 2011.
[11] Y. Nakai *et al.*, "High-speed microscopy with an electrically tunable lens to image the dynamics of *in vivo* molecular complexes," *Rev. Sci. Instrum.*, vol. 86, no. 1, p. 013707, 2015.
[12] C. Zuo, Q. Chen, W. Qu, and A. Asundi, "High-speed transport-of-intensity phase microscopy with an electrically tunable lens," *Opt. Exp.*, vol. 21, no. 20, pp. 24060–24075, 2013.
[13] L. Dong, A. K. Agarwal, D. J. Beebe, and H. Jiang, "Adaptive liquid microlenses activated by stimuli-responsive hydrogels," *Nature*, vol. 442, no. 7102, pp. 551–554, 2006.
[14] L. Dong, A. K. Agarwal, D. J. Beebe, and H. Jiang, "Variable-focus liquid microlenses and microlens arrays actuated by thermoresponsive hydrogels," *Adv. Mater.*, vol. 19, no. 3, pp. 401–405, 2007.
[15] X. Zeng, C. Li, D. Zhu, H. J. Cho, and H. Jiang, "Tunable microlens arrays actuated by various thermo-responsive hydrogel structures," *J. Micromech. Microeng.*, vol. 20, no. 11, p. 115035, 2010.
[16] A. Katsuyuki, "Embodiment 1," Japanese Patent 8–292 374, Nov. 5, 1996.

Aditi Kanhere received the B.S. degree in electronics and telecommunication engineering from the University of Pune, Maharashtra, India, in 2009, and the Ph.D. degree in electrical engineering from the University of Wisconsin–Madison, USA, in 2015. She is currently with Digilens Inc., CA, USA. Her other research interests include optical imaging, lens design, camera calibration, and holography.

Guangyun Lin received the Ph.D. degree from Zhongshan University, Guangzhou, China, in 1997. She was a Faculty Member with Zhongshan University, Guangzhou, China, from 1992 to 1998. She was a Postdoctoral Research Associate with the Boyce Thompson Institute, Cornell University, Ithaca, NY, USA, from 1998 to 2001. She was a Scientist with Invitrogen Life Technology, Carlsbad, CA, USA, from 2001 to 2004. She is currently an Associate Scientist with the Department of Bacteriology, and the Department of Electrical and Computer Engineering, University of Wisconsin–Madison, WI, USA. She has been with the University of Wisconsin–Madison since 2005. Her research interests focus on molecular biology study of C. botulinum toxins and their complex, and biosensing technologies.

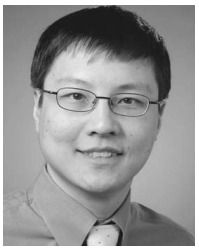

Hongrui Jiang received the B.S. degree in physics from Peking University, Beijing, China, and the M.S. and Ph.D. degrees in electrical engineering from Cornell University, Ithaca, NY, in 1999 and 2001, respectively. From 2001 to 2002, he was a Postdoctoral Researcher with the Berkeley Sensor and Actuator Center, University of California at Berkeley. He is currently the Vilas Distinguished Achievement Professor and a Lynn H. Matthias Professor in Engineering with the Department of Electrical and Computer Engineering, a Faculty Affiliate with the Department of Biomedical Engineering, and the Department of Materials Science and Engineering, and a Member of the McPherson Eye Research Institute with the University of Wisconsin–Madison. His research interests are in microfabrication technology, biological and chemical microsensors, microactuators, optical microelectromechanical systems, smart materials and micro-/nanostructures, lab-on-chip, and biomimetics and bioinspiration. He is a Member of the Editorial Board of the IEEE/ASME JOURNAL OF MICROELECTROMECHANICAL SYSTEMS. He is a Fellow of the Institute of Physics, the Royal Society of Chemistry, and the American Institute for Medical and Biological Engineering. He was a recipient of the National Science Foundation CAREER Award and the Defense Advanced Research Projects Agency Young Faculty Award in 2008, the H. I. Romnes Faculty Fellowship of the University of Wisconsin–Madison in 2011, the National Institutes of Health Director's New Innovator Award in 2011, and the Vilas Associate Award of the University of Wisconsin in 2013.